Environ. Sci. Technol. 1997, 31, 3086–3092

RWLP0244

Gas/Particle Partitioning of Semivolatile Organic Compounds To Model Inorganic, Organic, and Ambient Smog Aerosols

CIKUI LIANG AND JAMES F. PANKOW*

Department of Environmental Science and Engineering, Oregon Graduate Institute, P.O. Box 91000, Portland, Oregon 97291-1000

JAY R. ODUM† AND JOHN H. SEINFELD‡

Department of Environmental Engineering Science and Department of Chemical Engineering, California Institute of Technology, Pasadena, California 91125

Gas/particle (G/P) partitioning is an important process that affects the deposition, chemical reactions, long-range transport, and impact on human and ecosystem health of atmospheric semivolatile organic compounds (SOCs). Gas/particle partitioning coefficients (K_p) were measured in an outdoor chamber for a group of polynuclear aromatic hydrocarbons (PAHs) and *n*-alkanes sorbing to three types of model aerosol materials: solid ammonium sulfate, liquid dioctyl phthalate (DOP), and secondary organic aerosol (SOA) generated from the photooxidation of whole gasoline vapor. K_p values were also measured for ambient *n*-alkanes sorbing to urban particulate material (UPM) during summer smog episodes in the Los Angeles metropolitan area. Based on the K_p values obtained for the aerosols studied here, for environmental tobacco smoke (ETS), and for a quartz surface, we conclude that G/P partitioning of SOCs to UPM during summer smog episodes is dominated by absorption into the organic fraction in the aerosol. Comparisons of the partitioning of SOCs to three different types of aerosols demonstrate that (1) DOP aerosol may be a good surrogate for ambient aerosol that consists mainly of organic compounds from primary emissions; (2) ETS particles may be a good surrogate for SOA; and (3) the sorption properties of ambient smog aerosol and the chamber-generated SOA from gasoline are very similar. The similarities observed between ambient smog aerosol and chamber-generated SOA from gasoline support the use of literature SOA yield data from smog chamber studies to predict the extent of SOA formation during summer midday smog episodes.

Introduction

Gas/particle (G/P) partitioning is an important process that affects the deposition, chemical reactions, long-range transport, and human and ecosystem health effects of atmospheric semivolatile organic compounds (SOCs). Much of the thinking about the G/P partitioning of SOCs has involved the assumption that the partitioning process involves simple physical adsorption (*1*–*3*). While this sorption mechanism will be important when atmospheric particulate material is comprised solely of mineral materials, urban particulate material (UPM) generally contains a significant amount of amorphous organic carbon (*4*, *5*). Thus, it seems likely that absorptive partitioning must be playing at least some role in urban air and also in air affected by urban sources.

An equation that has been used successfully to parameterize G/P partitioning is (*2*, *6*, *7*)

$$K_p = \frac{F/\mathrm{TSP}}{A} \tag{1}$$

where K_p ($m^3/\mu g$) is the G/P partitioning coefficient for a given compound; F and A are the P- and G-phase concentrations (ng/m^3) of the compound, respectively; and TSP ($\mu g/m^3$) is the total suspended particulate material concentration. When both *ad*sorptive and *ab*sorptive partitioning are operative, K_p can be parameterized as (*8*)

$$K_p = \frac{C_1 + C_2}{p_L^\circ} \tag{2}$$

where p_L° (torr) is the pure compound subcooled liquid vapor pressure. The terms C_1/p_L° and C_2/p_L° represent the adsorptive and absorptive contributions to K_p, respectively. Detailed theoretical expressions for C_1 and C_2 are given by Pankow (*8*). Within a given compound class (*e.g.*, polycyclic aromatic hydrocarbons (PAHs), *n*-alkanes, etc.), C_1 and C_2 will be only weakly compound dependent, and log $(F/\mathrm{TSP})/A$ values will tend to be correlated with log p_L° according to

$$\log K_p = m_r \log p_L^\circ + b_r \tag{3}$$

where m_r is usually near −1.

The temperature dependence of K_p for a given compound sorbing to a given type of atmospheric particulate material can be expressed as (*2*, *8*)

$$\log K_p = m_p/T + b_p \tag{4}$$

Most of the temperature dependence explicitly present in eq 4 is implicitly present in eq 3 due to the temperature dependence of p_L°.

Based on a comparison of organic matter-phase-normalized K_p values that were measured for PAHs partitioning to environmental tobacco smoke (ETS) and estimated for partitioning to UPM, Liang and Pankow (*9*) have suggested that absorption may frequently be the dominant G/P partitioning mechanism for SOCs in urban air. In addition, Odum *et al.* (*10*) recently showed from smog chamber studies that the condensation of the photooxidation products which form secondary organic aerosol (SOA) is very well described by an absorptive G/P partitioning model. In this paper, we discuss smog chamber experiments that were performed to examine the partitioning of two classes of SOCs (PAHs and *n*-alkanes) to three different model aerosol materials: solid ammonium sulfate; nonpolar, liquid dioctyl phthalate (DOP); and polar, amorphous SOA generated from the photooxidation of whole gasoline vapor. G/P partitioning was also measured for UPM collected during two heavy smog episodes in the Los Angeles metropolitan area at a sampling site in the city of Pasadena. The UPM data were then compared to the data for the model aerosols to obtain information about both the operative G/P partitioning mechanism during summer smog episodes and the nature of UPM.

Experimental Section

Smog Chamber Experiments. Five experiments were conducted in the Caltech 60-m^3 flexible Teflon smog chamber

* Corresponding author phone: 503-690-1080; fax: 503-690-1556; e-mail: pankow@ese.ogi.edu.
† Department of Environmental Engineering Science.
‡ Department of Chemical Engineering.

S0013-936X(97)00252-6 CCC: $14.00 © 1997 American Chemical Society

PM3006519177

Source: https://www.industrydocuments.ucsf.edu/docs/lmgj0001

described in detail elsewhere (*10*–*12*). Prior to each experiment, the chamber was flushed with 4–5 bag volumes of purified compressed air while being allowed to warm to 31–38 °C under sunlight for at least 12 h. The purified compressed air was obtained by passing laboratory compressed air through four consecutive packed sorbent beds that contained (in order) Purafil, Drierite, 13X molecular sieve, and activated charcoal. After purification but before entering the chamber, the air was rehumidified to a relative humidity (RH) of approximately 10% for the chamber temperature of 31–36 °C using distilled/deionized water. The warm temperatures prevented the use of higher RH values because such use would have led to condensation in the sample lines between the chamber and the instrumentation.

Solid, inorganic aerosol was generated by atomizing an aqueous solution of 5 g/L ammonium sulfate using a stainless steel, constant rate atomizer (*10*). Before entering the Teflon chamber, the aerosol was passed via heated copper tubing first through a diffusional dryer packed with indicating silica gel and then through a ^{85}Kr charge neutralizer. The initial number concentration in the chamber was $\sim 7 \times 10^4/cm^3$. The geometric mean diameter was 111 ± 1.5 nm.

Liquid DOP aerosol was generated by atomizing a 0.005% by weight solution of DOP in pentane using a stainless steel, constant rate atomizer. Before entering the Teflon chamber, the DOP aerosol was passed through a diffusional dryer packed with activated charcoal to remove pentane, then through a ^{85}Kr charge neutralizer. The initial number concentration in the chamber was $\sim 10^4/cm^3$. The geometric mean diameter was 480 ± 1.6 nm.

Amorphous SOA was generated by first adding seed $(NH_4)_2SO_4$(s) particles at a concentration in the chamber of $10^4/cm^3$ (total aerosol volume ~20 $\mu m^3/cm^3$). These particles served as condensation nuclei. The chamber was then covered with a black tarpaulin so that photochemical reactions would not begin until all reactants had been added and given time to become well mixed. This was followed by injections of propene, NO, and NO_2 into the chamber to obtain initial concentrations of 300, 640, and 340 ppbv, respectively. These chemicals led to the generation of sufficient hydroxyl radicals and ozone to sustain the subsequent photochemical reactions. SOA was generated using "industry-average" gasoline obtained from the Auto/Oil Air Quality Research Improvement Program (*13*). A total of 700 μL of the gasoline was completely volatilized in a glass dilution bulb that was gently heated while being purged with purified lab air that was in turn directed into the chamber through Teflon lines. The initial total carbon concentration in the chamber was 9000 $\mu g/m^3$. Convective mixing, advective mixing caused by wind agitation of the chamber walls, and diffusion were allowed to mix the chamber for 20 min. The tarpaulin was then removed to initiate the photooxidation. After 2 h, the photochemical reactions were halted by covering the chamber again with the tarpaulin. Approximately 500–600 $\mu g/m^3$ of SOA (total aerosol volume of 500–600 $\mu m^3/cm^3$ and geometric mean diameter of 520 ± 1.2 nm) and more than 1 ppm of ozone was generated during this period. This ozone was titrated down to a concentration of 150 ppbv by slowly vaporizing 330 μL of liquid tetramethylethylene into the chamber. This precaution was taken in order to avoid excessive destruction of the SOC model compounds, which were added next. Most of the SOCs were added by injecting ~300 μL of a 250 ng/μL per component mixture of PAHs and *n*-alkanes in methylene chloride through a hot (300 °C) injector located at the base of the chamber. Two *n*-alkanes (C_{16} and C_{17}) were added to the chamber by injecting individual 50-μL aliquots of these compounds at $\sim 10^4$ ng/μL in methylene chloride.

Sampling of the SOCs was commenced approximately 1 h after their injection into the chamber. Available information on G/P partitioning kinetics (*14*) suggests that this was long enough to allow G/P equilibrium to be reached. G- and P-phase organic compounds were collected through a copper tube (i.d. = 0.5 in.) that extended ~30 cm into the chamber. Sampling event durations and conditions are listed in Table 1. The sampler utilized a 102 mm diameter glass fiber filter (GFF) (with an identical backup filter) to collect P-phase organic compounds. The data obtained with the backup filter were used to correct for the adsorption of G-phase SOCs to the front filter as described for quartz filters by Hart and Pankow (*15*). (On average, the mass of a compound of interest found on the backup QFF was ~15% of that on the front QFF; no compound dependence was observed in this number.) Following the filters, two parallel trains were used to collect G-phase compounds. One train employed two sequential adsorption/thermal desorption (ATD) cartridges containing ~1 g each of Tenax-GC to collect the more volatile compounds. The second train employed two sequential 198 cm^3 polyurethane foam (PUF) plugs to collect the less volatile compounds. The GFFs were precleaned by baking at 370 °C overnight and then held at room temperature in a desiccator containing indicating silica gel prior to sampling. The PUF plugs were Soxhlet-extracted with methylene chloride for 24 h before use. Each ATD cartridge was cleaned by pumping 1 L of 1:1 hexane:acetone through the cartridge at 2 mL/min, purged with ultra-pure helium at 50 °C for 20 min to remove the solvents, then conditioned at 300 °C for 2 h with a 1 mL/min flow of ultra-pure helium. During sampling, the flow rates were: filters, 70.8; Tenax-GC train, 0.324; and PUF train, 70.8 L/min, respectively. The face velocity for the filters was 18.5 cm/s.

TABLE 1. Sampling Data for Collection of Ambient and Smog Chamber Aerosols

event	date	sampling period (min)	temp (°C)	TSP ($\mu m/m^3$)
smog ambient (low-vol)	08/01/96	235	37	114
smog ambient (low-vol)	08/14/96	240	37	106
smog ambient (high-vol)	08/12/96	240	37	104
gasoline SOA, chamber	08/02/96	30	31	540
gasoline SOA, chamber	08/07/96	65	31	394
DOP, chamber	08/05/96	60	36	210
DOP, chamber	08/14/96	60	36	460
$(NH_4)_2SO_4$(s), chamber	08/09/96	90	32	109

The TSP was measured for each experiment by collecting particles with a 47-mm Teflon-coated GFF (tc-GFF) at a flow rate of 30 L/min for 20 min. Before use, each tc-GFF was Soxhlet-extracted with methylene chloride for 12 h, air-dried at room temperature, and then kept in a Petri dish prior to sampling. The tc-GFFs were weighed both before and after sampling. In each case, prior to weighing, the tc-GFFs were held for 1 h at 23 °C and 40% RH.

Complete aerosol number and size distribution measurements were recorded for every smog chamber experiment with a 1-min sampling frequency using a TSI (St. Paul, MN) Model 3071 cylindrical scanning electrical mobility spectrometer (SEMS) equipped with a TSI Model 3760 condensation nuclei counter. This equipment was housed in an enclosed cart maintained at 25 °C and located directly adjacent to the chamber. The SEMS system was operated with sheath and excess flows of 2.5 L/min, and inlet and classified aerosol flows of 0.25 L/min to allow for the measurement of aerosol size distributions in the 30–850 nm range. The aerosol size distribution data were used to provide independent measures of the TSP values.

Ambient Aerosol Sampling. Low-volume sampling was performed on the roof of Keck Laboratory during two separate smog episodes. The same equipment and filter type employed to sample the smog chamber were used. The sampling period for both episodes was 12 PM to 4 PM. The average RH for

PM3006519178

Source: https://www.industrydocuments.ucsf.edu/docs/lmgj0001

TABLE 2. Measured Log K_p Values for Different Types of Aerosols

compound	log p_L° (torr)[a]	log K_p ($m^3/\mu g$)
$(NH_4)_2SO_4$(s), Chamber (32 °C and 10% RH)		
heptadecane C_{17}	−3.07	−4.48
octadecane C_{18}	−3.57	−4.06
nonadecane C_{19}	−4.06	−4.04
eicosane C_{20}	−4.55	−3.58
heneicosane C_{21}	−5.04	−2.76
docosane C_{22}	−5.53	−2.30
tetracosane C_{24}	−6.51	−1.23
fluorene	−1.91	−5.48
phenanthrene	−2.74	−4.46
anthracene	−2.76	−4.52
fluoranthene	−3.87	−3.31
pyrene	−4.05	−3.27
Ambient Smog,[b] Ambient (37 °C and 42% RH)		
octadecane C_{18}	−3.31	−5.07
eicosane C_{20}	−4.23	−4.36
heneicosane C_{21}	−4.71	−4.01
docosane C_{22}	−5.18	−3.55
tetracosane C_{24}	−6.13	−2.11
DOP,[c] Chamber (36 °C and 10% RH)		
hexadecane C_{16}	−2.45	−4.81
heptadecane C_{17}	−2.93	−4.32
heneicosane C_{21}	−4.86	−2.34
docosane C_{22}	−5.34	−1.58
tetracosane C_{24}	−6.30	−1.24
fluorene	−1.80	−4.95
phenanthrene	−2.62	−4.23
anthracene	−2.65	−4.31
fluoranthene	−3.74	−2.82
pyrene	−3.92	−2.80
Gasoline SOA,[d] Chamber (31 °C and 10% RH)		
hexadecane C_{16}	−2.63	−5.53
heptadecane C_{17}	−3.12	−4.79
octadecane C_{18}	−3.62	−4.36
nonadecane C_{19}	−4.11	−3.71
eicosane C_{20}	−4.61	−3.70
heneicosane C_{21}	−5.10	−2.59
docosane C_{22}	−5.60	−2.72
tetracosane C_{24}	−6.58	−1.06
pentacosane C_{25}	−7.08	−0.44
naphthalene	−0.21	−6.28
acenaphthene	−1.58	−6.10
fluorene	−1.95	−5.58
phenanthrene	−2.78	−4.57
anthracene	−2.80	−4.01
fluoranthene	−3.92	−3.30
pyrene	−4.10	−3.15
chrysene	−5.34	−1.07

[a] Log p_L° values are temperature corrected. [b] Log K_p values are the averages for the 08/01/96 and 08/14/96 experiments. [c] Log K_p values are the averages for the 08/05/96 and 08/14/96 experiments. [d] Log K_p values are the averages for the 08/02/96 and 08/07/96 experiments.

the two days was 42%. Other sampling information is given in Table 1. The GFFs were weighed before and after sampling as with the tc-GFFs in the chamber experiments.

A single high-volume aerosol sample for carbon analysis and specific surface area measurement was taken at the same location from 12 PM to 4 PM during a third smog episode. An 8 × 10 in. quartz fiber filter (QFF) was used to collect particles at a flow rate of 1.4 m^3/min. The QFF was precleaned by baking overnight at 370 °C and then held at room temperature in a desiccator containing indicating silica gel until used. After sampling, a portion of the QFF was analyzed for inorganic carbon (IC), elemental carbon (EC), and organic carbon (OC) by Sunset Laboratory (Forest Grove, OR). Total carbon (TC) was taken to be the sum IC + EC + OC. Another portion of the QFF was sent to Micromeritics (Norcross, GA) for specific surface area measurements.

TABLE 3. Summary of Slopes (m_r) and Intercepts (b_r) for Log K_p vs Log p_L° Correlation Lines

aerosol type	m_r	b_r
PAHs		
$(NH_4)_2SO_4$(s) (t = 32 °C and RH 10%)	−1.04	−7.41
DOP (t = 36 °C and RH 10%)	−1.09	−7.02
gasoline SOA (t = 31 °C and RH 10%)	−1.05	−7.24
ETS[a] (t = 20 °C and RH 60%)	−1.02	−6.90
***n*-Alkanes**		
$(NH_4)_2SO_4$(s) (t = 32 °C and RH 10%)	−0.96	−7.66
DOP (t = 36 °C and RH 10%)	−0.98	−7.15
gasoline SOA (t = 31 °C and RH 10%)	−1.09	−8.37
ambient smog (t = 37 °C and RH 42%)	−1.03	−8.68
ETS[a] (t = 20 °C and RH 60%)	−0.89	−7.44

[a] Data are from ref 9.

Analytical Procedures. After sampling, each ATD cartridge was capped, sealed in a screw cap culture tube, and kept at −25 °C until analyzed. Each ATD cartridge was analyzed by thermal desorption with capillary GC/MS as described elsewhere (*16*). Immediately after sampling, each PUF plug and each GFF was spiked with surrogate standard compounds (acenaphthene-d_{10}, phenanthrene-d_{10}, and chrysene-d_{12}) and then Soxhlet-extracted overnight with 400 and 250 mL, respectively, of methylene chloride. PUF and GFF blanks were also extracted for each experiment. The extracts were concentrated down to ~30 mL by rotary evaporation and then kept at −25 °C until analyzed. Prior to GC/MS analysis, each extract was blown down to ~100 μL with N_2, weighed, and then spiked with internal standard compounds (naphthalene-d_8, anthracene-d_{10}, and perylene-d_{12}). Each extract was analyzed using GC/MS with a splitless injection of 1 μL. A 30-m, 0.32 mm i.d., 0.25 μm film thickness DB-5 capillary column (J&W Scientific, Folsom, CA) was used. The GC temperature program used was as follows: hold at 50 °C for 2 min, 50−100 °C at 25 °C/min, 100−300 °C at 10 °C/min, and then hold at 300 °C for 2 min. On average, recoveries for acenaphthene-d_{10}, phenanthrene-d_{10}, and chrysene-d_{12} were 93.3 ± 6.1, 93.7 ± 3.8, and 96.4 ± 5.4, respectively.

Results and Discussion

Adsorptive Partitioning to $(NH_4)_2SO_4$(s) Aerosol. If adsorption is the dominant partitioning mechanism, a surface-area-normalized constant $K_{p,s}$ can be defined as (*17*)

$$K_{p,s}\ (m^3/m^2) = \frac{K_p}{a_{TSP}\ 10^{-6} g/\mu g} \qquad (5)$$

where a_{TSP} (m^2/g) is the specific surface area of the adsorbing solid. In this case, eq 3 can be rewritten as

$$\log K_{p,s} = m_{r,s} \log p_L^\circ + b_{r,s} \qquad (6)$$

where $m_{r,s} = m_r$ and $b_{r,s} = b_r - \log (a_{TSP}/10^6)$.

Table 2 gives the log K_p values for the PAHs and *n*-alkanes for sorption to $(NH_4)_2SO_4$(s) aerosol. Table 3 provides the corresponding m_r and b_r values. Log $K_{p,s}$ values were calculated by normalizing the measured K_p values with a_{TSP} according to eq 5. The value of a_{TSP} was estimated to be 17.5 m^2/g by assuming that the $(NH_4)_2SO_4$(s) particles were spherical with a density of 1.77 g/cm^3. It is well known that the partitioning of organic compounds to inorganic surfaces is RH-dependent (*17, 18*) and that the sorption usually becomes stronger as the RH decreases. Since the partitioning experiments performed in the chamber with $(NH_4)_2SO_4$(s) were conducted at the relatively low RH of 10% and since the ambient smog *n*-alkane data were collected at RH 42%, extrapolations of the $(NH_4)_2SO_4$(s) log $K_{p,s}$ values to RH 42% were necessary to permit a comparison of the two data sets.

PM3006519179

Source: https://www.industrydocuments.ucsf.edu/docs/lmgj0001

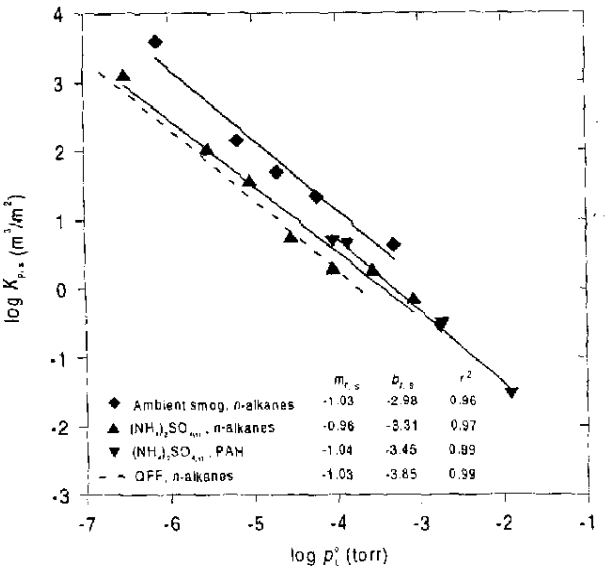

FIGURE 1. Comparison of log $K_{p,s}$ vs log p_L° correlations among different types of aerosols at RH 42%. QFF (quartz fiber filter) data are from Storey *et al.* (17).

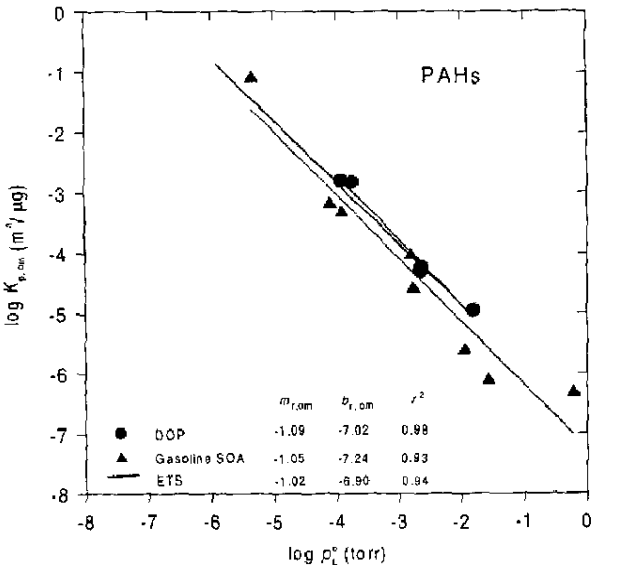

FIGURE 2. Comparison of log $K_{p,om}$ vs log p_L° for PAHs among different types of organic aerosols. ETS data are from Liang and Pankow (9).

Because of the presence of sorbed water on inorganic surfaces even at relatively low RH values, the adsorption of nonpolar organic gases has been found to be fundamentally similar for a range of inorganic surfaces including quartz, silica, and clay (*19*). We will therefore assume that adsorption to $(NH_4)_2SO_4$(s) particle surfaces is similar to adsorption to quartz surfaces. Storey *et al.* (*17*) have provided a detailed examination of the RH dependence of the adsorption of a range of PAHs and *n*-alkanes to a quartz surface. The needed compound-specific extrapolations were therefore based on the 30−70% RH data of Storey *et al.* (*17*). It was assumed that (1) only $b_{r,s}$ is a function of RH and (2) the change in $b_{r,s}$ with RH for $(NH_4)_2SO_4$(s) is similar to that for quartz. The extrapolated compound-dependent increases in log $K_{p,s}$ for quartz between RH 42% and RH 10% were therefore subtracted from the log $K_{p,s}$ values for $(NH_4)_2SO_4$(s) obtained in this study. The results are plotted in Figure 1. The a_{TSP}-normalized ambient smog *n*-alkane data are also plotted in Figure 1. Sheffield and Pankow (*20*) have reported that a_{TSP} = 2.1 m^2/g for UPM collected during the summer in Portland, OR. Corn *et al.* (*21*) reported that a_{TSP} = 1.9 m^2/g for UPM collected during the summer in Pittsburgh, PA. These values are consistent with measurements made in this study. Therefore, the value of a_{TSP} for the ambient smog sample in this study was taken to be 2.0 m^2/g.

Normalizing ambient smog aerosol log K_p values by an estimate of a_{TSP} allows one to test whether adsorption is an important partitioning mechanism for UPM. As seen in Figure 1, the calculated log $K_{p,s}$ values for the *n*-alkanes sorbing to the ambient smog samples at RH 42% are much larger than those for sorption to $(NH_4)_2SO_4$(s) aerosol as extrapolated to RH 42%. (A similar comparison for the PAHs is not possible because the PAH concentrations were too low to be quantified accurately with the methods used.) Considering that the inorganic portion of the midday smog aerosol was probably well represented by $(NH_4)_2SO_4$(s), we conclude that adsorption to inorganic surfaces probably cannot account for the sorption of the *n*-alkanes observed in the ambient samples. This suggests that adsorption was not the operative mechanism controlling the partitioning of SOCs to these ambient smog aerosol samples and that the log $K_{p,s}$ values calculated for the *n*-alkanes sorbing to these samples are not physically meaningful quantities.

Absorptive Partitioning to Organic Aerosols. When absorption into a liquid (or at least amorphous) organic matter (om) phase is the dominant sorption mechanism, an om-phase-normalized constant $K_{p,om}$ can be defined as (*10*, *22*)

$$K_{p,om} = \frac{K_p}{f_{om}} \tag{7}$$

where f_{om} is the weight fraction of the TSP that comprises the om phase. In this case, eq 3 can be rewritten as

$$\log K_{p,om} = m_{r,om} \log p_L^\circ + b_{r,om} \tag{8}$$

where $m_{r,om} = m_r$ and $b_{r,om} = b_r - \log f_{om}$. Based on theory developed by Pankow (*8*), it can be shown that (*22*)

$$K_{p,om} = \frac{760RT}{M_{om}\zeta p_L^\circ 10^6} \tag{9}$$

where M_{om} is the number-averaged molecular weight of the om phase, ζ is the mole fraction scale activity coefficient of the compound of interest in that phase, and R is the gas constant (8.206 × 10^{-5} m^3 atm mol^{-1} K^{-1}).

The measured log K_p values for the liquid DOP aerosol and the amorphous SOA generated from the photooxidation of whole gasoline are given in Table 2. The corresponding log K_p vs log p_L° correlation parameters are given in Table 3. The log $K_{p,om}$ vs log p_L° plots are given in Figures 2 and 3. Also given are the regression lines for the partitioning of PAHs and *n*-alkanes to environmental tobacco smoke (ETS) as determined by Liang and Pankow (*9*). For the DOP, SOA, and ETS aerosols, f_{om} was taken to be 1.0, yielding $K_p = K_{p,om}$. For the ambient smog samples, the carbon analyses revealed that the amount of IC in those samples was essentially zero so that TC = OC + EC. On average, TC constituted 21% of the TSP, with 87% of the TC being organic (OC/EC = 6.7). When all the aerosol is secondary in nature, Izumi and Fukuyama (*23*) have found that the mass of the om phase is 2.0 times the mass of total OC mass alone assuming that the density of om is 1.0 g/cm^3. On the other hand, when most of the primary organic aerosol in LA in the summertime is coming from diesel exhaust and meat cooking (*24*), then most of the carbon is heavy alkanes and aldehydes. For these kinds

PM3006519180

Source: https://www.industrydocuments.ucsf.edu/docs/lmgj0001

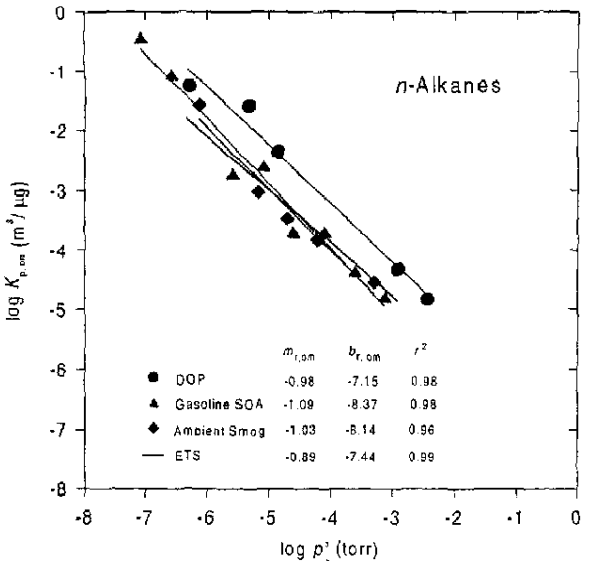

FIGURE 3. Comparison of log $K_{p,om}$ vs log p_L° for *n*-alkanes among different types of organic aerosols. ETS data are from Liang and Pankow (9). The f_{om} values for the DOP, gasoline SOA, ambient smog, and ETS aerosols were taken to be 1.0, 1.0, 0.29, and 1.0, respectively.

of aerosol, the mass of the om phase is 1.2 times the mass of total OC alone (25). In this context, allowing for the presence of other elements in the organic matrix (*e.g.*, hydrogen and oxygen, including that in the water in the om phase), the mass of the om phase in Los Angeles aerosol was taken to be 1.6 times the mass of the total OC mass alone since 53−58% of the total OC was estimated to be secondary in nature for our ambient smog samples (see text below). These considerations lead to the estimate $f_{om} = 0.29$ for the ambient smog samples. This value was used with eq 8 and the assumption that the partitioning to the ambient smog was absorptive in nature to calculate log $K_{p,om}$ values for the ambient smog samples. The results are plotted in Figure 3.

The slopes and intercepts for the three regression lines in Figure 2 were compared using the "analysis of covariance" method described by Snedecor and Cochran (26). The slopes of the three regression lines in Figure 2 are all close to −1 and not significantly different (95% confidence level). This indicates that within each of the three organic aerosols phases, ζ remained approximately constant for the range of PAHs of interest for a given RH. The intercepts of the three regression lines in Figure 2 are moreover not significantly different (95% confidence level), indicating that the factor $M_{om}\zeta$ is approximately the same for the three organic aerosols considered. The partitioning of the *n*-alkanes to the organic aerosols is considered in Figure 3. On average, the partitioning of the *n*-alkanes to the organic aerosols was found to be weaker than that of the PAHs. For the *n*-alkanes, the partitioning was found to be similar for the gasoline SOA, ambient smog, and ETS aerosols. Within this group, the slopes of log $K_{p,om}$ vs log p_L° regression lines are all close to −1, and both the slopes and intercepts are not significantly different (95% confidence level) with the analysis of covariance. The sorption of the *n*-alkanes to the DOP aerosol, however, was much stronger than to the other three aerosols. Since it is very likely that M_{DOP} was larger than the M_{om} values for the other aerosols, the increase of partitioning was probably due to ζ values for the *n*-alkanes that were significant lower (and closer to 1) in the DOP aerosol as compared to the other aerosol phases.

During summer smog episodes in the South Coast Air Basin, a significant fraction of the ambient organic aerosol is often of secondary origin (27−32). Using data from Claremont, CA, Turpin and Huntzicker (32) suggested a method to estimate the secondary OC content based on the total OC (= $OC_{pri} + OC_{sec}$) and a derived correlation between OC_{pri} and EC. For our ambient smog samples, by assuming that the OC_{pri}/EC ratio for Pasadena was similar to that observed by Turpin and Huntzicker (32) in Claremont, we estimate that 53−58% of total OC was secondary in origin. Therefore, because the anthropogenic volatile organic gas profile in the South Coast Air Basin is very similar to that of whole gasoline vapor (33), it does seem likely that the SOA generated in the basin was similar to the SOA that was generated from whole gasoline in the smog chamber as suggested by Figure 3. Furthermore, the similarity indicates that it may be valid to extrapolate SOA yield data from smog chamber studies (10) to predict the extent of SOA formation during summer midday smog episodes.

O'Brien *et al.* (34) have reported that mono- and dicarboxylic acids make up an appreciable portion (22% and 10%, respectively) of the organic content of particulate material found under photochemical smog conditions in the Los Angeles area. Schuetzle *et al.* (35) have found high concentrations of organic alcohols and difunctional organic compounds in SOA. Based on the significant organic content of the ambient smog samples examined here, it is likely that the polarities of the om-portion of the ambient smog aerosol and the SOA generated from gasoline were much higher than the polarity of the DOP aerosol. Moreover, because of the presence of the two long alkane chains in DOP molecules, DOP aerosols are likely to be more hospitable to *n*-alkanes, the ζ values for the *n*-alkanes in DOP are expected to be closer to 1.0 as well as lower than in the other aerosol phases.

The overall spread in the log K_p vs log p_L° correlation lines in Figure 3 is greater than that in Figure 2. This result may be the consequence of a greater sensitivity in the absorptive uptake of *n*-alkanes to changes in the polarity of the om-phase than is the case for the PAHs. It would be useful to know all of the M_{om} values for the organic aerosols studies here so that this hypothesis could be tested directly by calculating the average ζ values for the PAHs and *n*-alkanes for each different aerosol type. (Methods for estimating ζ values in liquid mixture of known composition are also available (36−38).) Unfortunately, the only M_{om} value that is known with some certainty at the present time is M_{DOP}, though it may be possible to estimate the molecular weight properties of diesel particle (39), smoke aerosol (40), atmospheric fine particle (41, 42), and secondary aerosol (34, 35). For DOP, we note that the solubility of DOP in water is only 3 mg/L at 25 °C (43). Since the mutual solubilities of water and organic compounds are well correlated (44), it can be concluded that the solubility of water in DOP will also be fairly low. Because the RH in the chamber experiments was only ~10%, it is very reasonable to assume that M_{DOP} was very close to the molecular weight of pure DOP, namely, 390 g/mol. When log $p_L^\circ = -3$, the regression parameters in Table 3 for DOP give log $K_{p,om} = -3.75$ and −4.21 for the PAHs and the *n*-alkanes, respectively. These values yield $\zeta = 0.28$ and 0.8, respectively. These results are consistent with literature values for ζ in DOP. In particular, the ζ values for benzene and octane in DOP have been reported to be 0.57 (60 °C) and 1.4 (120 °C) (45).

While it is instructive as well as useful to have a detailed understanding of the individual values of ζ and M_{om} for a given compound or class of compounds sorbing to a given organic aerosol, there will be many circumstances for which knowledge of the product of $M_{om}\zeta$ alone will be sufficient. In this context, we note that the sorption properties of ETS and the SOA generated from gasoline were very similar, both for the PAHs and *n*-alkanes. This suggests that ETS may be a useful surrogate phase for SOA. It may therefore be possible to use ETS and the methods of Liang and Pankow (9) to

PM3006519181

Source: https://www.industrydocuments.ucsf.edu/docs/lmgj0001

estimate the log $K_{p,om}$ values for SOA for other classes of compounds (*e.g.*, organic alcohols and carboxylic acids). Similarly, DOP aerosol may be a useful surrogate for ambient organic aerosol that consists mainly of moderately nonpolar organic compounds of primary emission origin (*e.g.*, diesel aerosol, which is about 50% organic carbon on average (*46*)).

In summary, we conclude that the G/P partitioning of SOCs to UPM containing a significant fraction of secondary organic carbon will be dominated by absorptive partitioning. This finding is consistent with the conclusions of Liang and Pankow (9) for UPM. This suggests that G/P partitioning in urban environments is correctly described by eqs 7–9 and supports the absorptive model for SOA formation proposed by Odum *et al.* (*10*).

Acknowledgments

This work was supported in part by the U.S. Environmental Protection Agency's Office of Exploratory Research (U.S. EPA/OER) under Grant R822312-01-0. This work was also supported in part by the U.S. Environmental Protection Agency Center on Airborne Organics under Grant R-819714-01-0, National Science Foundation Grant ATM-9307603, the Coordinating Research Council, and the Chevron Corporation. We gratefully acknowledge the technical assistance of Timothy P. W. Jungkamp, Robert J. Griffin, Lorne M. Isabelle, and Wentai Luo in the design, sampling preparation, and analysis phases of the experimental work. We also appreciate Martha J. Shearer and Paul G. Tratnyek for their helpful suggestions on the statistical analysis of the data. Finally, the authors would like to thank Donna Reed for assisting with many details associated with the shipment of the sampling equipment.

Glossary

A	gas-phase concentration of a compound (ng/m^3)
a_{TSP}	specific surface area of suspended particles (m^2/g)
APM	atmospheric particulate material
b_r	intercept in a plot of log K_p vs log p_L°
$b_{r,om}$	intercept in a plot of log $K_{p,om}$ vs log p_L°
$b_{r,s}$	intercept in a plot of log $K_{p,s}$ vs log p_L°
DOP	dioctyl phthalate
EC	elemental carbon (μg/cm^2)
ETS	environmental tobacco smoke
F	particulate-phase concentration of compound (ng/m^3)
f_{om}	weight fraction of the TSP that comprises the om phase
GFF	glass fiber filter
IC	inorganic carbon (μg km^2)
K_p	gas/particle partitioning coefficient (m^3/μg)
$K_{p,om}$	om-phase-normalized gas/particle partitioning constant (m^3/μg)
$K_{p,s}$	surface-area-normalized gas/particle partitioning constant (m^3/m^2)
M_{DOP}	number-averaged molecular weight of the DOP phase (g/mol)
M_{om}	number-averaged molecular weight of the om phase (g/mol)
m_r	slope in a plot of log K_p vs log p_L°
$m_{r,om}$	slope in a plot of log $K_{p,om}$ vs log p_L°
$m_{r,s}$	slope in a plot of log $K_{p,s}$ vs log p_L°
OC	organic carbon (μg/cm^2)
OC_{pri}	primary organic carbon
OC_{sec}	secondary organic carbon
om	organic matter
p_L°	vapor pressure of pure subcooled liquid (torr)
ppbv	part per billion (10^9) by volume
QFF	quartz fiber filter
R	gas constant (= 8.206×10^{-5} m^3 atm mol^{-1} K^{-1})
RH	relative humidity
SOA	secondary organic aerosol
SOCs	semivolatile organic compounds
T	temperature (K)
TC	total carbon (μg/cm^2)
tc-GFF	Teflon-coated glass fiber filter
TSP	concentration of total suspended particulate material (μg/m^3)
UPM	urban particulate material
ζ	mole fraction scale activity coefficient of a compound in organic matter phase

Literature Cited

(1) Junge, C. E. In *Fate of Pollutants in the Air and Water Environments*; Suffet, I. H. Ed.; Wiley: New York, 1977; pp 7–26.
(2) Yamasaki, H.; Kuwata, K.; Miyamoto, H. *Environ. Sci. Technol.* **1982**, *16*, 189–194.
(3) Pankow, J. F. *Atmos. Environ.* **1987**, *21*, 2275–2283.
(4) Gray, H. A.; Cass, G. R.; Huntzicker, J. J.; Heyerdahl, E. K.; Rau, J. A. *Sci. Total Environ.* **1984**, *36*, 17–25.
(5) Shah, J. J.; Johnson, R. L.; Heyerdahl, E. K.; Huntzicker, J. J. *JAPCA* **1986**, *36*, 254–257.
(6) Pankow, J. F. *Atmos. Environ.* **1991**, *25A*, 2229–2239.
(7) Pankow, J. F. *Atmos. Environ.* **1992**, *26A*, 2489–2497.
(8) Pankow, J. F. *Atmos. Environ.* **1994**, *28*, 185–188.
(9) Liang, C. K.; Pankow, J. F. *Environ. Sci. Technol.* **1996**, *30*, 2800–2805; 3650 (errata).
(10) Odum, J. R.; Hoffmann, T.; Bowman, F.; Collins, D.; Flagan, R. C.; Seinfeld, J. H. *Environ. Sci. Technol.* **1996**, *30*, 2580–2585.
(11) Pandis, S. N.; Paulson, S. E.; Seinfeld, J. H.; Flagan, R. C. *Atmos. Environ.* **1991**, *25A*, 997–1008.
(12) Wang, S. C.; Paulson, S. E.; Grosjean, D.; Flagan, R. C.; Seinfeld, J. H. *Atmos. Environ.* **1992**, *26A*, 403–420.
(13) Hochhauser, A. M.; Benson, J. D.; Burns, V. R.; Gorse, R. A.; Koehl, W. J.; Painter, L. J.; Ribbon, B. H.; Reuter, R. M.; Rutherford, J. A. *SAE Technical Paper No. 912322*; Society of Automotive Engineers: Warren PA, 1991.
(14) Kamens, R.; Odum, J. R.; Fan, Z. *Environ. Sci. Technol.* **1995**, *29*, 43–50.
(15) Hart, K. M.; Pankow, J. F. *Environ. Sci. Technol.* 28, 655–661.
(16) Rounds, S. A.; Tiffany, B. A.; Pankow, J. F. *Environ. Sci. Technol.* **1993**, *27*, 366–377.
(17) Storey, J. M.; Luo, W. T.; Isabelle, L. M.; Pankow, J. F. *Environ. Sci. Technol.* **1995**, *29*, 2420–2428.
(18) Goss, K. U. *Environ. Sci. Technol.* **1992**, *26*, 2287–2294.
(19) Goss, K. U. *Environ. Sci. Technol.* **1994**, *28*, 640–645.
(20) Sheffield, A. E.; Pankow, J. F. *Environ. Sci. Technol.* **1994**, *28*, 1759–1766.
(21) Corn, M.; Montgomery, T. L.; Esmen, N. A. *Environ. Sci. Technol.* **1971**, *5*, 155–158.
(22) Pankow, J. F. In *Gas and Particle Partitioning Measurements of Atmospheric Organic Compound*; Lane D. A., Ed.; Gordon and Breach: Newark, NJ, in press.
(23) Izumi, K.; Fukuyama, T. *Atmos. Environ.* **1990**, *24A*, 1433–1441.
(24) Schauer, J. J.; Rogge, W. F.; Hidlemann, L. M.; Mazurek, M. A.; Cass, G. R. *Atmos. Environ.* **1996**, *30*, 3837–3855.
(25) Countess, R. J.; Wolff, G. T.; Cadle, S. H. *J. Air Pollut. Control Assoc.* **1980**, *30*, 1194–1200.
(26) Snedecor, G. W.; Cochran, W. G. *Statistical Methods*, 8th ed.; Iowa State University Press: Ames, IA, 1989.
(27) Gartrell, G., Jr.; Friedlander, S. K. *Atmos. Environ.* **1975**, *9*, 279–299.

PM3006519182

Source: https://www.industrydocuments.ucsf.edu/docs/lmgj0001

(28) Grosjean, D.; Friedlander, S. K. *J. Air Pollut. Control Assoc.* **1975**, *25*, 1038−1044.
(29) Larson, S. M.; Cass, G. R.; Gray, H. A. *Aerosol Sci. Technol.* **1989**, *10*, 118−130.
(30) Turpin, B. J.; Huntzicker, J. J. *Atmos. Environ.* **1991**, *25A*, 207−215.
(31) Pandis, S. N.; Harley, R. A.; Cass, G. R.; Seinfeld, J. H. *Atmos. Environ.* **1992**, *26A*, 2269−2282.
(32) Turpin, B. J.; Huntzicker, J. J. *Atmos. Environ.* **1995**, *29*, 3527−3544.
(33) Harley, R. A.; Hannigan, M. P.; Cass, G. R. *Environ. Sci. Technol.* **1992**, *26*, 2395−2408.
(34) O'Brien, R. J.; Crabtree, J. H.; Holmes, J. R.; Hoggan, M. C.; Bockian, A. H. *Environ. Sci. Technol.* **1975**, *9*, 577−582.
(35) Schuetzle, D.; Cronn, D.; Crittenden, A. L.; Charlson, R. J. *Environ. Sci. Technol.* **1975**, *9*, 838−845.
(36) Fredenslund, A.; Jones, R. L.; Prausnitz, J. M. *AIChE J.* **1975**, *21*, 1086−1099.
(37) Gmehling, J. *Fluid Phase Equilibr.* **1986**, *30*, 119−134.
(38) Fredenslund, A.; Sorensen, J. M. In *Models for Thermodynamic and Phase Equilibria Calculations*; Sandler, S. I., Ed; Marcel Dekker: New York, 1994; pp 287−361.
(39) Rogge, W. F.; Hidlemann, L. M.; Mazurek, M. A.; Cass, G. R. *Environ. Sci. Technol.* **1993**, *27*, 636−651.
(40) bin Abas, M. R.; Simoneit, B. R. T.; Elias, V.; Cabral, J. A.; Cardoso, J. N. *Chemosphere* **1995**, *30*, 995−1015.
(41) Hidlemann, L. M.; Markowski, G. R.; Cass, G. R. *Environ. Sci. Technol.* **1991**, *25*, 744−759.
(42) Fraser, M. P.; Grosjean, D.; Grosjean, E.; Rasmussen, R. A.; Cass, G. R. *Environ. Sci. Technol.* **1996**, *30*, 1731−1743.
(43) Wolfe, N. A.; Steen, W. C.; Burns, L. A. *Chemosphere* **1980**, *3*, 403−408.
(44) Pankow, J. F. *Aquatic Chemistry Concepts*; Lewis Publishers: Chelsea, MI, 1991; pp 335−338.
(45) Tiges, D.; Gmehling, J.; Medina, A.; Soares, M.; Bastos, J.; Alessi, P.; Kikic, I. *Activity Coefficients at Infinite Dilution*, Vol. IX, Part I; Dechema: Germany, 1986.
(46) Japar, S. M.; Szkariat, A. C.; Gorse, R. A., Jr.; Heyerdahl, E. K.; Johnson, R. L.; Rau, J. A.; Huntzicker, J. J. *Environ. Sci. Technol.* **1984**, *28*, 231−234.

Received for review March 19, 1997. Revised manuscript received June 30, 1997. Accepted July 23, 1997.[⊗]

ES9702529

[⊗] Abstract published in *Advance ACS Abstracts*, September 1, 1997.

PM3006519183

Source: https://www.industrydocuments.ucsf.edu/docs/lmgj0001